Implementing the Keldysh formalism into the *ab initio* Gaussian Embedded Cluster Method for the calculation of quantum transport

E. Louis,[1,2] J. A. Vergés,[3] J. J. Palacios,[1,2] A. J. Pérez-Jiménez,[4] and E. SanFabián[2,4]

[1]*Departamento de Física Aplicada, Universidad de Alicante, San Vicente del Raspeig, Alicante 03690, Spain.*
[2]*Unidad Asociada del Consejo Superior de Investigaciones Científicas, Universidad de Alicante, San Vicente del Raspeig, Alicante 03690, Spain.*
[3]*Departamento de Teoría de la Materia Condensada, Instituto de Ciencia de Materiales de Madrid (CSIC), Cantoblanco, Madrid 28049, Spain.*
[4]*Departamento de Química-Física, Universidad de Alicante, San Vicente del Raspeig, Alicante 03690, Spain.*

We discuss the key steps that have to be followed to calculate quantum transport out of equilibrium by means of the *ab initio* Gaussian Embedded Cluster Method recently developed by the authors. Our main aim is to emphasize through several examples that, if a sufficiently large portion of the electrodes is included in the *ab initio* calculation, which does also incorporate an electrochemical potential difference $\mu_L - \mu_R = eV$, there is no need to impose an electrostatic potential V drop accross the system.

PACS numbers: 73.63.Fg, 71.15.Mb

The effort devoted to investigate electronic transport through molecular bridges and metallic nanocontacts has sharply increased in recent years[1,2,3]. In particular, a variety of *ab initio* methods are being developed aiming to catch the essentials of these systems[4,5,6,7,8,9,10]. These methods share most of the ingredients [Landauer-Keldysh formalism for transport and density functional (DF) theory], but differ in their numerical implementation, which translates into their computational efficiency and predictibility power. A critical problem not yet fully solved is the way these methods actually deal with out-of-equilibrium transport[11,12,13]. Most of the approaches that are being proposed impose from the outset an external and uniform electrostatic potential drop across the molecule or nanocontact[6,8,9]. The latter is justified when considering planar electrodes, which in most cases do not correspond to experimental electrode geometries. This choice simplifies the numerical implementation, but can condition the outcome of the calculation. In this work we discuss how the Keldysh formalism can be implemented into *ab initio* transport schemes and, in particular, into the Gaussian Embedded Cluster Method (GECM) recently developed by the authors[14,15]. Conclusive numerical evidence is presented which shows that, if a sufficiently large portion of the electrodes is incorporated into the *ab initio* calculations, there is no need to add an external electrostatic potential to the self-consistent potential. This provides a natural, consistent, way of solving the electrostatic problem for generic electrode geometries.

In a single-particle description, inherent to DF calculations, one obtains the current I through the molecule or nanocontact at non-zero temperature and finite bias voltage V by integrating the transmission probability:

$$I = \frac{e}{h}\int_{-\infty}^{\infty} T(E,V)[f(E-\mu_L) - f(E+\mu_R)]\mathrm{d}E, \quad (1)$$

where $f(E-\mu_{\mathrm{L,R}})$ is the Fermi distribution for the left and right electrodes whose electrochemical potentials are denoted by μ_{L} and μ_{R}, respectively, and $\mu_{\mathrm{L}} - \mu_{\mathrm{R}} = eV$. The transmission coefficient $T(E,V)$ depends both on temperature and the applied bias, and is given by

$$T(E,V) = \mathrm{Tr}[\hat{\Gamma}_{\mathrm{L}}\hat{G}^{(+)}\hat{\Gamma}_{\mathrm{R}}\hat{G}^{(-)}], \quad (2)$$

where hats denote operators. The Green function operators and the gamma operators depend on energy and the applied potential (both arguments dropped for convenience). The latter are defined as $\hat{\Gamma}_{\mathrm{L,R}} = \hat{\Sigma}^{(+)}_{\mathrm{L,R}} - \hat{\Sigma}^{(-)}_{\mathrm{L,R}}$, where $\hat{\Sigma}_{\mathrm{L,R}}$ denotes the self-energy operator for the part of the right and left semi–infinite electrodes which is not included in the *ab initio* calculation. The Green function operator is in its turn defined as

$$\left[(E \pm i\delta)\hat{I} - \hat{F} - \hat{\Sigma}^{(\pm)}_L - \hat{\Sigma}^{(\pm)}_R\right]\hat{G}^{(\pm)} = \hat{I}, \quad (3)$$

where $\hat{I}$ is the unity operator. On the other hand, the density matrix out of equilibrium is obtained from[16]

$$P_{\alpha\beta} = -\frac{i}{2\pi}\int_{-\infty}^{\infty}\mathrm{d}E\sum_{\gamma\delta}\left[S^{-1}_{\alpha\gamma}G^{<}_{\gamma\delta}S^{-1}_{\delta\beta}\right] \quad (4)$$

where $G^{<}_{\gamma\delta}$ are the matrix elements in a non-orthogonal basis of the lesser Green function operator given by

$$\hat{G}^{<} = i\hat{G}^{(+)}\left[f(E-\mu_L)\hat{\Gamma}_{\mathrm{L}} + f(E-\mu_R)\hat{\Gamma}_R\right]\hat{G}^{(-)}. \quad (5)$$

Most of the technical difficulties implicit in the evaluation of the above expressions have been discussed in previous works[6,8,9,15]. There is, however, an important conceptual issue that, in our opinion, remains unsolved and worth clarifying. In the presence of a voltage difference between electrodes one might be tempted to impose from

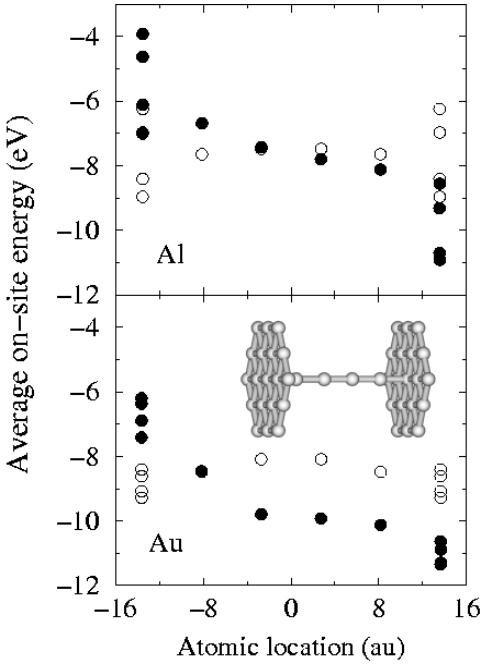

FIG. 1: Average onsite energies of the atomic orbitals versus atomic position in $M19-M4-M19$ nanocontacts (two 19 atom (111)-planes plus a four atom chain, see inset). The results correspond to V=0 (empty circles) and 5 V (filled circles) and $M \equiv$Al (a) and Au (b).

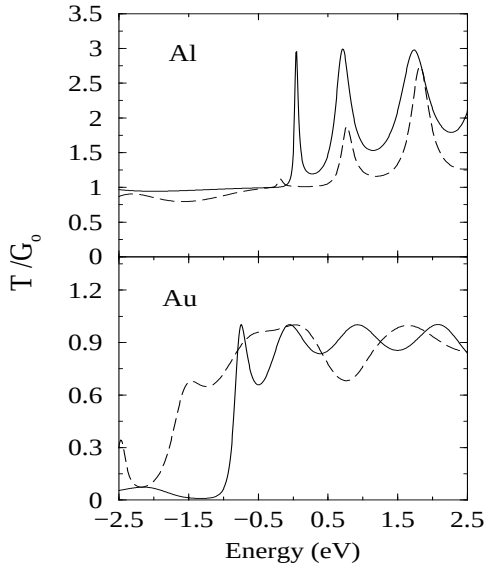

FIG. 2: Transmission versus energy for V=0 (continuous line) and 5 V (dashed line) in the $M19-M4-M19$ nanocontacts of Figure 1, with $M \equiv$Al (a) and Au (b), are shown.

the outset an external electrostatic potential drop across the molecule or nanocontact. As the potential profile depends strongly on the electrode geometry, one would have to solve Poisson equation with the boundary conditions appropriate for such geometry. A way around this problem is to assume a simple form for the electrodes[6,8,9]. However, adding an external potential through the homogeneous solution of the Poisson equation is unnecessary if a significant part of the metallic electrodes has already been included in the initial cluster and an *electrochemical potential difference* is maintained. The difference between left and right electrochemical potentials charges one electrode and discharges the other one, effectively creating an electrostatic potential drop across the constriction[17]. In general, once self-consistency is attained, an electrostatic potential difference V between atoms one or two layers inside opposite electrodes develops while they remain neutral. On the other hand, the potential difference between atoms on the surface of opposite electrodes is smaller than V since they carry the charges. In summary, we assume all the charges responsible for the electrostatic potential across the constriction to be part of our cluster instead of imposing a usually unknown external electrostatic potential. For a large enough number of atoms in the electrodes this should be essentially correct.

The way we have actually implemented this self-contained, out-of-equlibrium scheme into the GECM initially proposed in Ref. 14 and later fully developed in Ref. 15 is hereafter described. A first step consists in carrying out a DF calculation by means of the GAUSSIAN98 code[18] of the region that contains the molecule or the set of atoms that form the contact between the electrodes plus *a significant part of the electrodes*. Once a reasonable accuracy has been achieved, the Green function for the infinite system is calculated and the density matrix given by Eq. 4 used in the subsequent DF process. The infinite electrode selfenergies are calculated by means of the Bethe lattice approximation and a minimal basis set with pseudopotentials was used in the calculations [see Ref. 15 for details]. In previous works, the DF calculations were carried out by means of the Becke three-parameter hybrid functional plus the correlation functional of Lee, Yang and Parr (B3LYP)[19]. A difficulty specific to the out-of-equilibrium case comes from the fact that the density matrix in Eq. 4 is complex. This can be handled in two ways: i) treating exchange within DF, instead of carrying out a full Hartree-Fock calculation (this can be easily done by using BLYP instead of B3LYP), and ii) incorporating the complex density matrix into the GAUSSIAN98 code. In the present case we have chosen the former as the second procedure would have required major changes in the standard code[20]. In order to get reasonably reliable results for finite bias, a root mean square error in the density matrix better than 10^{-4} was mandatory.

Calculations have been carried out for gold and aluminum nanocontacts similar to those of the insets in Figures 1 and 3. Two types of fcc clusters have been considered: (a) two (111) planes containing 19 atoms each plus a four atom chain labeled $M19-M4-M19$ (a capacitor was described by taking out the four atom chain

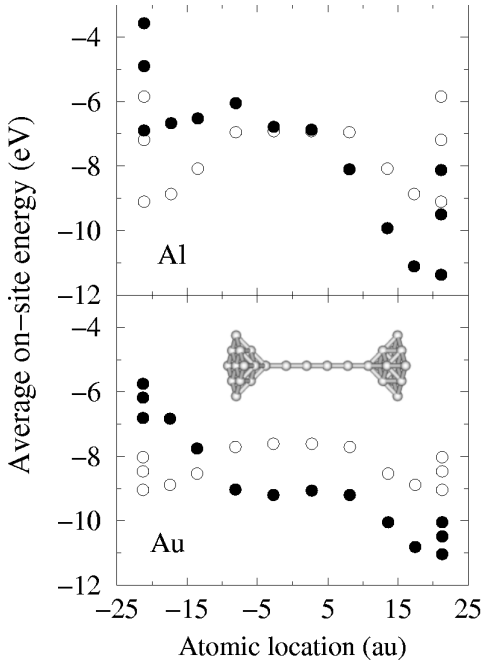

FIG. 3: Same as Figure 1 for a (100) pyramidal arrangement (two pyramids containing 14 atoms each plus a four-atom chain; see inset) referred to as $M14-M4-M14$ (see text).

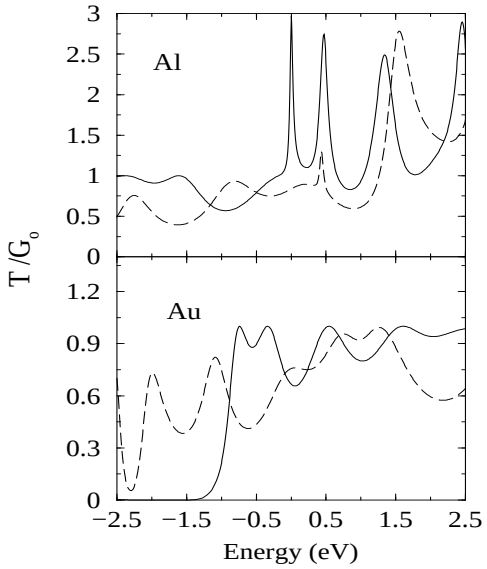

FIG. 4: Transmission versus energy for V=0 (continuous line) and 5 V (dashed line) in the $M14-M4-M14$ nanocontacts of Figure 3, with M= Al (a) and Au (b).

leaving a wide gap between the planes); (b) two (100)-oriented pyramidal clusters plus a 4 atom chain labeled $M14-M4-M14$ [(100)-oriented pyramidal nanocontacts as $M5-M5$, $M14-M14$ and $M30-M30$ have also been considered]. Interatomic bulk distances have been taken for the whole cluster (2.86 $\AA$ for Al and 2.88 $\AA$ for Au). All results correspond to zero temperature and an external bias voltage in the range 0-5 V. The structural stability of the system models is an important issue when one is interested in the interpretation of experimental results. This is not the case here.

Figure 1 shows the average on-site energies ($5d6s6p$ for Au and $3s3p$ orbitals for Al) on all atoms of the nanocontacts $M19-M4-M19$ for zero and 5 V bias. This magnitude reflects only the electrostatic potential on each atom, not telling us anything about the chemical potential (charge) on them. The on-site energies in the planes are less dispersed in the case of gold than in aluminum. This is probably due to the simple s-character of the wavefunctions at the Fermi level that gold has (as opposed to the sp character in aluminum). At 5 V bias, the major drop in the potential occurs at the chain/plane contacts. While the total potential drop in gold (aluminum) is 4.44 eV (4.6 eV) the drop between the first and the last chain atoms is only 1.67 eV (1.43 eV). In the case of zero bias, the results are symmetric with respect to the geometric center of symmetry, as expected. Instead, a similar symmetry is absent for 5 V. Namely, whereas the potential drop between the left electrode and the first atom in the chain is 1.92 eV (1.69 eV) for gold (aluminum) nanocontacts, it is only of 0.85 eV (1.48 eV) between the chain end and the right electrode. This feature seems common to all previously reported results and reflects not only bulk band structure features, but also details of the nanocontact geometry (see below). The transmission for $V = 0$ and 5 V is shown in Figure 2. There are noticeable differences both in gold and aluminum. In the latter the peak structure is significantly changed, whereas in gold the gap below -0.5 eV is partially filled. It is worth noting that although the total current calculated by integrating in a window [$-V/2, V/2$] the transmission for V=0 does not differ much from that obtained with the full non-equilibrium approach (more important changes are expected in complex molecules), the differential conductance is significantly different.

The average on-site energies on all atoms of the nanocontacts $M14-M4-M14$ for zero and 5 V bias, are depicted in Figure 3. As above, the on-site energies in the outer planes are less dispersed in the case of gold than in aluminum. Now the potential drop along the chain is significantly different for the two metals: while in the case of gold the total potential drop is 4.29 eV and the drop between the first and the last chain atoms is only 0.162 eV, in aluminum these numbers change to 4.56 and 2.043, respectively. These results support our claim in the sense that what matters are not only the bulk features of the metals but also the nanocontact geometry. The asymmetry in the potential drop remarked above is also noted. Again, the differences in the transmission between zero and 5 V bias are significant. The peak structure in aluminum is noticeably reduced and the gap in gold filled over a range larger than 1 eV.

In Table I we report the fittings of the numerical re-

TABLE I: Fittings of the numerical results for the variation with applied electrostatic potential V of the difference between the average on-site energies of the atomic orbitals at the outer planes in clusters similar to those of Figures 1 and 2 (see text) and of current through them, with functions $\Delta E = aV^b$ and $I/G_0 = cV^d$, respectively (ΔE, I/G_0 and V given in eV, G_0 being the quantum of conductance $2e^2/h$).

cluster	a	b	c	d
$Al5-Al5$	0.820	0.979	0.810	1.039
$Al14-Al14$	0.882	0.992	0.807	1.08
$Al30-Al30$	0.942	0.984	0.635	1.20
$Al14-Al4-Al14$	0.900	1.008	1.196	0.865
$Al19-Al4-Al19$	0.919	1.001	1.315	0.925
$Al19$-vacumm-$Al19$	0.953	1.001	-	-
$Au5-Au5$	0.803	0.935	0.521	1.068
$Au14-Au14$	0.840	0.993	0.668	1.067
$Au14-Au4-Au14$	0.882	0.971	0.805	0.950
$Au19-Au4-Au19$	0.882	1.003	0.886	0.91
$Au19$-vacumm-$Au19$	0.928	1.001	-	-

sults for the difference between the average energies of all atoms in the left and right planes in $M19-M4-M19$ nanocontacts, and the two outer planes in the pyramidal nanocontacts, versus the applied external potential. The fittings were done with aV^b, instead of assuming a linear relationship from the start. All regression coefficients were higher than 0.999. Although a and b are always rather close to 1, some significant features are worth of comment. There is a steady increase of a and b as the size of the outer planes increases. The values closest to one are found for the capacitors (the nanocontacts with a $\approx 14\mathring{A}$ gap). In the latter case the coefficient a is only 7% (5%) smaller than 1 for gold (aluminum) nanocontacts, while the exponent cannot in practice be differentiated from one. The small deviations with respect to the "ideal" behavior are due to the finite charge that those planes carry and/or to a yet insufficiently large electrode. As expected, in pyramidal nanocontacts the results steadily approach the ideal behavior as the size of the cluster increases. These results constitute the main message of the present work. The results for the current versus voltage were also fitted with $I/G_0 = bV^d$ (see Table I). In this case the lowest regression coefficient is 0.99 (in some cases the results are better fitted with second order polynomia). The significant deviations from a linear behavior (Ohm's law) are not surprising in systems as small as those investigated here and have been reported previously. The current is in general higher in aluminum than in gold, which is consistent with the larger conductance found for aluminum at the Fermi level[15]. Deviations from linearity are also more important in the case of aluminum, with the exponent increasing with the size of the pyramidal cluster. This is a consequence of a number of facts, including the increasing contributions from the π channel discussed in Ref. 15.

Summarizing, we have discussed the practical procedures one should follow to implement the non-equilibrium Keldysh formalism into the Gaussian Embedded Cluster Method previously developed by the authors. In our view the most important outcome of this work is the conclusive evidence concerning the need of incorporating a sufficiently large portion of the electrodes in the *ab initio* calculation. If this is done, the artificial addition of an applied external potential to the potential in the Schrödinger equation is unnecessary.

Partial financial support by the spanish MCYT (grants BQU2001-0883, PB96-0085, and MAT03-04450-C03) and the Universidad de Alicante is gratefully acknowledged.

[1] C. Joachim, J. K. Gimzewski, and A. Aviram, Nature (London) **408**, 541 (2000).

[2] A. Nitzan, Annu. Rev. Phys. Chem. **52**, 681 (2001).

[3] N. Agrait, A. Levi-Yeyati, and J. van Ruitenbeek, to be published.

[4] N. D. Lang, Phys. Rev. B **52**, 5335 (1995).

[5] V. Mujica, A. Roitberg, and M. Ratner, J. Chem. Phys. **112**, 6834 (2000).

[6] J. Taylor, H. Guo, and J. Wang, Phys. Rev. B **63**, 245407 (2001).

[7] Y. Xue, S. Datta, and M. A. Ratner, arXiv:cond-mat/0112136.

[8] P. S. Damle, A. W. Ghosh, and S. Datta, Phys. Rev. B **64**, 201403 (2001).

[9] M. Brandbyge, J. L. Mozos, P. Ordejón, J. Taylor, and K. Stokbro, Phys. Rev. B **65**, 165401 (2002).

[10] P. Damle, A. Ghosh, and S. Datta, arXiv:cond-mat/0206551.

[11] L. V. Keldysh, Sov. Phys. JETP **20**, 1018 (1965).

[12] Y. Meir and N. Wingreen, Phys. Rev. Lett. **68**, 2512 (1992).

[13] S. Hershfield, J. Davies, and J. Wilkins, Phys. Rev. Lett. **67**, 3720 (1991).

[14] J. J. Palacios, A. J. Pérez-Jiménez, E. Louis, and J. A. Vergés, Phys. Rev. B **64**, 115411 (2001).

[15] J. J. Palacios, A. J. Pérez-Jiménez, E. Louis, E. SanFabián, and J. A. Vergés, Phys. Rev. B **66**, 035322 (2002).

[16] An error, recurrent in the literature, consists of writing the elements of the density matrix without the overlap matrices that appear in Eq. (5). This error is compensated by the erroneous writing of the Green functions, say for instance the retarded as $G^{(+)}_{NO} = \left[(E+i\delta)S - F_{NO} - \Sigma^{(+)}_{NO}\right]^{-1}$, where $\Sigma^{(+)}_{NO}$ are the matrix elements of the operator $\hat{\Sigma}^{(+)} = \hat{\Sigma}^{(+)}_L + \hat{\Sigma}^{(+)}_R$ in a non-orthogonal (NO) basis. One can easily check by taking matrix elements in the operator equation (4) that, in a non-orthogonal basis, $G^{(+)}_{NO} = S\left[(E+i\delta)S - F_{NO} - \Sigma^{(+)}_{NO}\right]^{-1} S$.

[17] R. Landauer, IBM J. Res. Dev. **1**, 233 (1957).

[18] M. J. Frisch, G. W. Trucks, H. B. Schlegel, M. A. R. G. E. Scuseria, J. R. Cheeseman, V. G. Zakrzewski, J. A. Montgomery, Jr., R. E. Stratmann, J. C. Burant, et al., GAUSSIAN98, Revision A.7, Gaussian, Inc., Pittsburgh PA, 1998.

[19] A. Becke, J. Chem. Phys. **98**, 5648 (1993).

[20] Unfortunately, the complex version of the link 502 in the GAUSSIAN98 code, named link 503, is rather obsolete.